

## Orientation and Alkylation Effects on Cation- $\pi$ Interactions in Aqueous Solution

Mark J. Rashkin, Robert M. Hughes, Nathaniel T. Calloway, and Marcey L. Waters\*

Contribution from the Department of Chemistry, CB 3290, University of North Carolina, Chapel Hill, North Carolina 27599

Received January 9, 2004; E-mail: mlwaters@email.unc.edu

**Abstract:** We have investigated the orientation dependence of the cation- $\pi$  interaction between a phenyl ring and a pyridinium ring in the context of a flexible model system in water. Of the four possible positions of the pyridinium nitrogen, ipso, ortho, meta, and para, we found a variation in the interaction energy of about  $0.75 \text{ kcal mol}^{-1}$ , with the stacking of the ipso-pyridinium ring providing the strongest interaction. The observed stability is attributed to the maximization of the electrostatic interaction, minimization of rotamers, and possible differences in hydration phenomena arising from alkylation.

### Introduction

Cation- $\pi$  interactions<sup>1</sup> have generated significant interest due to their roles in protein structure,<sup>2</sup> biomolecular recognition,<sup>3</sup> and enzymatic catalysis.<sup>4</sup> The cation- $\pi$  interaction between a positively charged  $\pi$ -system and an aromatic ring, such as the interaction of arginine (Arg) with tryptophan (Trp), has been proposed to be particularly stabilizing due to the additional van der Waals and  $\pi$ - $\pi$  stacking components of the interaction.<sup>2</sup> Other cation- $\pi$  interactions involving positively charged  $\pi$ -systems may also be important in biomolecular recognition, such as the interaction of the pyridinium ring of  $\text{NAD}^+$  with Trp in the binding site of a protein<sup>3d</sup> and the stacking of positively charged alkylated DNA bases in excision-repair enzymes<sup>3c,4b</sup> and mRNA cap binding proteins.<sup>3c</sup>

Gellman and co-workers have shown that there is an orientation dependence on stacking interactions of neutral heteroaromatic rings,<sup>5</sup> which has relevance to base stacking. However, to our knowledge, the impact of orientation of the positive charge relative to the aromatic ring in a cation- $\pi$  interaction has not been investigated experimentally. In the system described here, we investigated the cation- $\pi$  interaction between a phenyl ring and a pyridinium ring in compounds **1a–d** in water and found that the orientation of the rings has a significant impact on the magnitude of the interaction and that alkylation of the pyridine ring can enhance the effect.

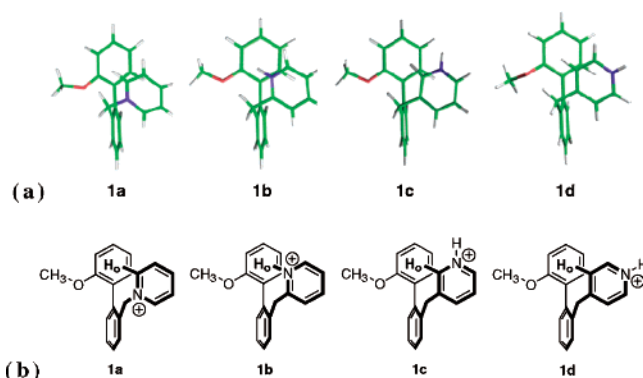


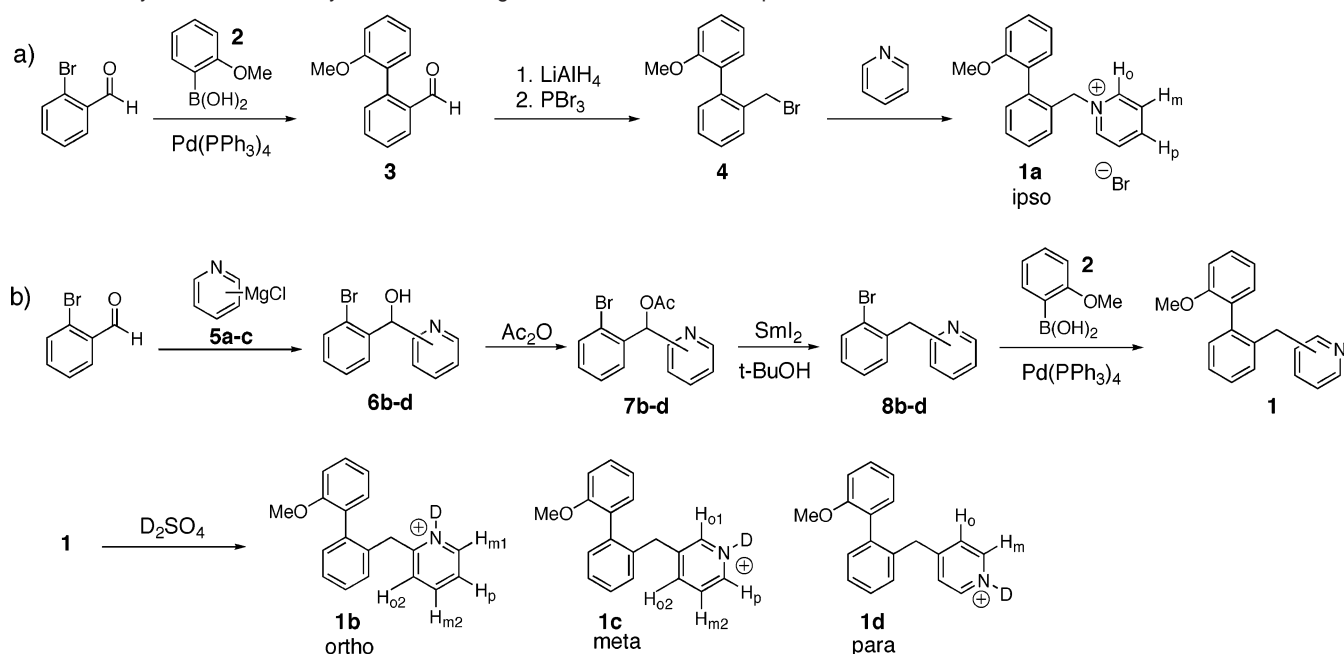
**Figure 1.** (a) Ab initio calculated structures of **1a–d** in explicit water (see Experimental Section). Green = carbon, blue = nitrogen, red = oxygen, white = hydrogen. (b) ChemDraw representation of compounds **1a–d**.

### Results and Discussion

**Design and Synthesis.** The model system is based on our previously reported system designed to examine offset stacked aromatic interactions.<sup>6</sup> As indicated by high level ab initio calculations in explicit water<sup>7</sup> (Figure 1), the system design allows for the pyridinium ring to stack against the top phenyl ring of the biaryl unit of compounds **1a–d** in an offset stacked conformation, placing the ortho-hydrogen of the pyridinium ring

- (1) (a) Ma, J. C.; Dougherty, D. A. *Chem. Rev.* **1997**, *97*, 1303–1324. (b) Castellano, R. K.; Diederich, F.; Meyer, E. A. *Angew. Chem., Int. Ed.* **2003**, *42*, 1210–1250.  
 (2) Gallivan, J. P.; Dougherty, D. A. *Proc. Natl. Acad. Sci. U.S.A.* **1999**, *96*, 9459–9464.  
 (3) (a) Zacharias, N.; Dougherty, D. A. *Trends Pharmacol. Sci.* **2002**, *23*, 281–287. (b) Muñoz-Caro, C.; Nino, A. *Biophys. Chem.* **2002**, *96*, 1–14. (c) Quioco, F. A.; Hu, G.; Gershon, P. D. *Curr. Opin. Struct. Biol.* **2000**, *10*, 78–86. (d) Yamamoto-Katayama, S.; Ariyoshi, M.; Ishihara, K.; Hirano, T.; Jingami, H.; Morikawa, K. *J. Mol. Biol.* **2002**, *316*, 711–723.  
 (4) (a) Lee, S.; Lin, X.; McMurray, J.; Sun, G. *Biochemistry* **2002**, *41*, 12107–12114. (b) Eichman, B. F.; O'Rourke, E. J.; Radicella, J. P.; Ellenberger, T. *Embo. J.* **2003**, *22*, 4898–4909.  
 (5) McKay, S. L.; Haptonstall, B.; Gellman, S. H. *J. Am. Chem. Soc.* **2001**, *123*, 1244–1245.

- (6) Rashkin, M. J.; Waters, M. L. *J. Am. Chem. Soc.* **2002**, *124*, 1860–1861.  
 (7) Frisch, M. J.; Trucks, G. W.; Schlegel, H. B.; Scuseria, G. E.; Robb, M. A.; Cheeseman, J. R.; Montgomery, J. A., Jr.; Vreven, T.; Kudin, K. N.; Burant, J. C.; Millam, J. M.; Iyengar, S. S.; Tomasi, J.; Barone, V.; Mennucci, B.; Cossi, M.; Scalmani, G.; Rega, N.; Petersson, G. A.; Nakatsuji, H.; Hada, M.; Ehara, M.; Toyota, K.; Fukuda, R.; Hasegawa, J.; Ishida, M.; Nakajima, T.; Honda, Y.; Kitao, O.; Nakai, H.; Klene, M.; Li, X.; Knox, J. E.; Hratchian, H. P.; Cross, J. B.; Adamo, C.; Jaramillo, J.; Gomperts, R.; Stratmann, R. E.; Yazyev, O.; Austin, A. J.; Cammi, R.; Pomelli, C.; Ochterski, J. W.; Ayala, P. Y.; Morokuma, K.; Voth, G. A.; Salvador, P.; Dannenberg, J. J.; Zakrzewski, V. G.; Dapprich, S.; Daniels, A. D.; Strain, M. C.; Farkas, O.; Malick, D. K.; Rabuck, A. D.; Raghavachari, K.; Foresman, J. B.; Ortiz, J. V.; Cui, Q.; Baboul, A. G.; Clifford, S.; Cioslowski, J.; Stefanov, B. B.; Liu, G.; Liashenko, A.; Piskorz, P.; Komaromi, I.; Martin, R. L.; Fox, D. J.; Keith, T.; Al-Laham, M. A.; Peng, C. Y.; Nanayakkara, A.; Challacombe, M.; Gill, P. M. W.; Johnson, B.; Chen, W.; Wong, M. W.; Gonzalez, C.; Pople, J. A. *Gaussian 98*, A11; Gaussian, Inc.: Pittsburgh, PA, 2003.

**Scheme 1.** Synthesis of Model Systems for Investigation of the Orientation Dependence of the Cation- $\pi$  Interaction

over the center of the phenyl ring. Hence, by varying the position of the nitrogen in the pyridinium ring, the overlap with the  $\pi$ -cloud of the anisole ring is systematically varied.

Compounds **1a–d** were synthesized as shown in Scheme 1. The synthesis of **1a** began with a Suzuki coupling of 2-bromobenzaldehyde and the boronic acid **2** to give compound **3** in 85% yield. This was followed by reduction of compound **3** with  $\text{LiAlH}_4$  and subsequent bromination with  $\text{PBr}_3$  to give compound **4** in a 75% overall yield for the two steps. The final product **1a** was obtained in quantitative yield as a white solid from reaction of **4** with pyridine.

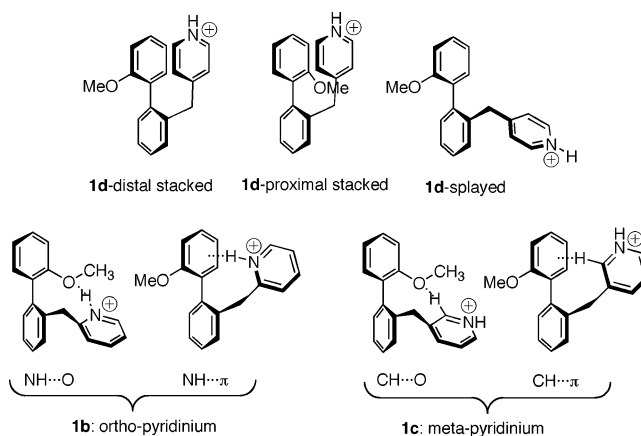
A representative synthetic route of **1b** began with the coupling of 2-pyridinylmagnesium chloride<sup>8</sup> and 2-bromobenzaldehyde to give **6a** in 52% yield. Compound **6a** was acylated with acetic anhydride followed by deoxygenation with samarium(II) iodide<sup>9</sup> to produce **8a**. Finally, Suzuki coupling of **8a** with **2** afforded the product **1b**.

**Conformational Analysis.** We performed ab initio calculations in explicit water which indicate that compounds **1a–d** populate a stacked geometry in which the methoxy group is distal to the pyridinium ring. Several other geometries are also accessible in this system (Figure 2). For example, the offset stacked geometry can occur either distal or proximal to the methoxy group or the pyridinium ring can swing away from the anisole ring, resulting in a splayed conformation. In some cases,  $\text{NH}\cdots\text{O}$ ,  $\text{NH}\cdots\pi$ , and  $\text{CH}\cdots\text{O}$  and  $\text{CH}\cdots\pi$  interactions may also be possible.<sup>10</sup>

NOE studies were performed to investigate the favored conformation of compounds **1a–d**. NOEs between the methoxy group and the pyridinium ring are expected for the proximal stacked geometry as well as the  $\text{NH}\cdots\text{O}$  and  $\text{CH}\cdots\text{O}$  interac-

**Table 1.** Upfield Shifting of the Pyridinium Ring Protons in Compounds **1a–d** and **N-Me-1b–d** Relative to Control Compounds **9a–d** and **N-Me-9b–d**

proton	$\Delta\delta$ (ppm)						
	<b>1a</b>	<b>1b</b>	<b>N-Me-1b</b>	<b>1c</b>	<b>N-Me-1c</b>	<b>1d</b>	<b>N-Me-1d</b>
$\text{H}_{\text{O}1}$	0.65			0.80	0.76	0.47	0.37
$\text{H}_{\text{O}2}$	0.65	0.37	0.51	0.56	0.44	0.47	0.37
$\text{H}_{\text{m}1}$	0.29	0.40	0.21			0.23	0.15
$\text{H}_{\text{m}2}$	0.29	0.25	0.27	0.27	0.20	0.23	0.15
$\text{H}_{\text{p}}$	0.17	0.23	0.16	0.18	0.17		
<i>N</i> -Me			0.37		0.20		0.09

**Figure 2.** Possible conformations of compounds **1a–d**.

tions. The fact that such NOEs are not observed suggests that that these geometries are not significantly populated in water. The lack of such NOEs is consistent with a distal stacked or splayed geometry.

Comparison of aromatic upfield shifts from **1a–d** to the corresponding unstacked control compounds **9a–d** (Figure 3) provides additional evidence for the offset stacked orientation of the pyridinium ring (Table 1). In each compound, all protons on the pyridinium ring are shifted upfield, supporting a stacked geometry as the favored conformation. In each case the ortho-hydrogens demonstrate the greatest upfield shifting, indicating

(8) Trecourt, F.; Breton, G.; Bonnet, V.; Mongin, F.; Marsais, F.; Queguiner, G. *Tetrahedron Lett.* **1999**, *40*, 4339–4342.

(9) Kato, Y.; Mase, T. *Tetrahedron Lett.* **1999**, *40*, 8823–8826.

(10) Similar  $\text{CH}\cdots\text{O}$  interactions between pyridinium CH groups and ether oxygens have been shown to be important to self-assembly in some organic solvents. (a) Houk, K. N.; Menzer, S.; Newton, S. P.; Raymo, F. M.; Stoddart, J. F.; Williams, D. J. *J. Am. Chem. Soc.* **1999**, *121*, 63, 1479–1487. (b) Raymo, F. M.; Houk, K. N.; Stoddart, J. F. *J. Org. Chem.* **1998**, *63*, 6523–6528.

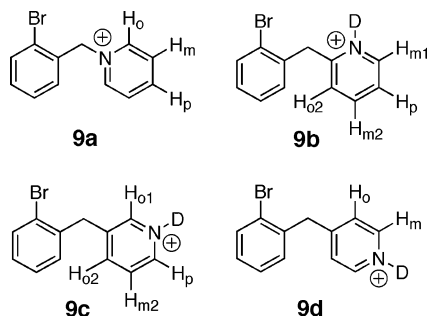


Figure 3. Control compounds **9a–d**.

Scheme 2. Stacked Conformation and Transition State of Compounds **1a–d**



that they are in closest proximity to the face of the ring. For example, the ortho-protons,  $H_o$ , of compound **1a** are shifted upfield 0.65 ppm, while  $H_m$  and  $H_p$  are only shifted 0.29 and 0.17 ppm, respectively. Moreover, alkylation of the nitrogen results in only minor changes in the upfield shifting, indicating that  $NH\cdots O$  and  $NH\cdots\pi$  interactions are not predominant, since methylation would disrupt these interactions. Upfield shifting of the *N*-methyl groups is also consistent with a stacked geometry for each compound (Table 1). The preference for the stacked geometry over other possible geometries is likely a result of both a hydrophobic component to the aromatic interaction and solvation of the ether oxygen and pyridinium NH by water. Nonetheless, it is clear that the position of the nitrogen in the ring influences the population of the stacked geometry, as the pyridinium ring in **1d** is not as shifted upfield as it is in **1a**.

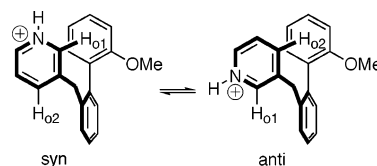
**Determination of Interaction Energies.** The 2'-methoxy group was incorporated to desymmetrize the biaryl unit and restrict rotation about the biaryl bond, resulting in diastereotopic methylene hydrogens. The relative strengths of the cation- $\pi$  interactions were determined by measuring the rate of rotation about the biaryl bond through dynamic NMR by fitting the line-broadened spectrum of the diastereotopic methylene protons,  $H_a$  and  $H_b$ , in  $D_2O$ , pH 1, as a function of temperature.<sup>11</sup> The fitting was accomplished using the program gNMR.<sup>12</sup> The accuracy of the analysis is dependent on a known baseline line width, which was provided by the unbroadened resonance of the methoxy group in this system. The strength of the interaction between the pyridinium and phenyl rings in this system is proportional to the difference in the ground state and transition state energies. Modeling of the transition state has indicated that the biaryl rings are coplanar and the pyridinium group is splayed, such that there is no interaction between the pyridinium ring and the phenyl ring in the transition state (Scheme 2). Therefore, any effect of the interaction between the pyridinium ring and phenyl ring on the rotational barrier in compounds **1a–d** may be attributed to differences in the ground-state energies.

Table 2. Barriers to Rotation of **1a–d** in  $D_2O$  (pH 1,  $D_2SO_4$ ) at 352 K<sup>a</sup>

compd	position	$\Delta G^\ddagger$ (kcal mol <sup>-1</sup> )	$\Delta\Delta G^\ddagger$ (kcal mol <sup>-1</sup> )
<b>1a</b>	ipso	18.48	-0.75
<b>1b</b>	ortho	18.08	-0.35
<b>1c</b>	meta	17.85	-0.12
<b>1d</b>	para	17.73	

<sup>a</sup> Propagation of errors gives an uncertainty of  $\pm 0.05$  kcal mol<sup>-1</sup>.

Scheme 3. Stacked Rotamers of **1c** in the Syn and Anti Conformations



The cation- $\pi$  interaction is believed to arise largely from an electrostatic interaction between a positive charge and the quadrupole moment of an aromatic ring.<sup>1</sup> Correspondingly, we expected **1b** to possess the strongest interaction and **1d** to possess the weakest interaction of the four compounds due to their differences in ability to access an optimal orientation between the positive charge and the center of the aryl ring.

Inspection of the rotational barriers in Table 2 indicates that there is a significant variation in the rotational barriers of **1a–d**, amounting to 0.75 kcal mol<sup>-1</sup>. Compound **1a** has the strongest interaction followed by **1b** then **1c** and **1d**. Inspection of the relative positions of the pyridinium nitrogen in Figure 1 provides insight into the order of stabilities of **1b–d**. Compound **1b** places the N–H directly over the phenyl ring, whereas the overlap of the N–H with the  $\pi$ -cloud is concomitantly less for **1c** and **1d**, resulting in an energetic variation of 0.35 kcal mol<sup>-1</sup>. However, it is not immediately obvious why the barrier of **1a** is significantly higher than that of **1b**.

There may be several factors that contribute to the larger interaction energy for compound **1a**. The electron-withdrawing cation in the ipso position polarizes the adjacent C–H bonds resulting in very electron poor ortho-hydrogens. Of the four compounds, **1a** is unique in the fact that both ortho-hydrogens are adjacent to the cation allowing both to receive maximum inductive effects. In contrast, both the ortho- and meta-pyridinium compounds, **1b** and **1c**, have two inequivalent stacked rotamers (Scheme 3). The rotational barrier is dependent on the relative populations of the syn and anti conformations. Comparison of upfield aromatic shifting provides a method for examining the stacked rotamer population. We compared **1b** and **1c** to their corresponding unstacked control compounds **9b** and **9c** (Table 1). As is evident by the difference in the upfield shifting of the nondegenerate ortho and meta protons, the syn population for **1b** and **1c** is 62% and 59%, respectively. Hence, the inequivalency of the two stacked rotamers results in a larger entropic cost for forming the preferred stacking interaction in **1b** and **1c** relative to **1a**.

The nature of the pyridinium nitrogen may also play a role in the difference in rotational barrier: the protonated nitrogen in **1b–d** may be involved in hydrogen bonding to the solvent which is not possible for the quaternary nitrogen in compound **1a**.<sup>13</sup> The hydrogen bonded water molecules may create a sphere of hydration that must be desolvated in order to access a cation- $\pi$

(11) Sandtröm, J. *Dynamic NMR Spectroscopy*; Academic Press: London, New York, 1982.

(12) gNMR, V. 3.6; Cherrwell Scientific Publishing.

(13) Meyer, S.; Louis, R.; Metz, B.; Agnus, Y.; Varnek, A.; Gross, M. *New J. Chem.* **2000**, *24*, 371–376.

interaction. Methylation of **1b–d** would allow the investigation of such a possibility. However, increased steric hindrance of an ortho-methylation makes comparison of the rotational barriers impossible. In addition, determination of the rotational barrier of *N*-methylated derivatives of **1c** and **1d** was not possible due to interference of the water peak in the NMR spectra at the reported temperatures. Nonetheless, we were able to compare the upfield shifting of **1b–d** to their *N*-methyl derivatives to determine the influence of methylation on the stacking interaction. In each case, the methylated compounds have similar, but not identical, upfield shifting of the pyridinium protons. Comparison of the syn/anti ratios for unmethylated and methylated compounds provides insight into the impact of methylation on the stacking interaction. For example, the syn/anti ratio for **1b** is 62:38 as determined from the meta-proton chemical shifts, whereas for *N*-Me-**1b** the ratio is 44:56. Hence, methylation actually favors the anti orientation, presumably for steric reasons, since the syn conformation would place the methyl group directly over the anisole ring. Comparison of **1c** to *N*-Me-**1c** provides insight into the contribution of alkylation in the stacking interaction in **1a**, since both **1a** and **1c** place a C–H group neighboring the nitrogen over the center of the anisole ring. The population of the syn conformation is 63% for *N*-Me-**1c**, as compared to 59% for **1c**, which amounts to approximately 0.1 kcal mol<sup>-1</sup> favoring the syn conformation when the nitrogen is methylated. Hence, the fact that **1a** is alkylated contributes to its enhanced stacking affinity but is not the sole source of the increased interaction energy.

## Conclusions

We have found a significant orientation dependence of on the cation- $\pi$  interaction between a pyridinium ring and phenyl ring. In this model system we have found that minimizing the number of different rotamers and maximizing the polarization of C–H bonds directly involved in the interaction with the  $\pi$ -system provide the strongest interaction. Alkylation of the nitrogen also enhances the interaction energy, depending on the geometry of interaction. These results demonstrate the sensitivity of cation- $\pi$  interactions to orientation and alkylation. Moreover, these studies demonstrate the ability to utilize cation- $\pi$  interactions to correctly orient guest molecules in molecular recognition systems. We expect these findings to increase the utility of cation- $\pi$  interactions as tools for molecular recognition.

## Experimental Section

**General.** All reagents and solvents were purchased from commercial sources and used without additional purification unless otherwise noted. Tetrahydrofuran and diethyl ether were dried via a column of neutral alumina under nitrogen prior to use.<sup>15</sup>

**Molecular Modeling.** Explicit water calculations were performed using Gaussian 98 (A 11).<sup>7</sup> For each molecule, all possible rotamers were constructed in Sybyl and placed in a droplet of 50 water molecules using the XFIT algorithm.<sup>15</sup> Structures were subsequently minimized for 5000 iterations using the Powell method with the Tripos force field and Gastieger–Huckel charges. Minimized, solvated structures were subsequently optimized using the ONIOM method as implemented in Gaussian 98 (A 11). In the ONIOM calculation, the molecule of interest was treated at the HF/6-31g\*\* level, and solvent molecules were treated with the UFF force field.

**Synthesis. A. 2-Methoxyphenylboronic Acid, 2.** A round-bottom flask charged with argon, anhydrous ether, and 2-bromoanisole (2.125 g, 11.36 mmol, 1.416 mL) was cooled to  $-78$  °C. *n*-BuLi (12.5 mmol, 5.1 mL, 2.5 M in hexanes) was added dropwise, and the solution was stirred for 1 h. The flask was then removed from the dry ice/acetone bath, and trimethylborate (12.5 mmol, 1.29 g, 1.31 mL) was added and allowed to warm to room temperature and stirred overnight. The reaction was quenched with 20 mL of 2 N HCl and stirred for 30 min followed by extraction into ether. The organic mixture was extracted with 20 mL of 1 N NaOH in two portions. The aqueous layer was washed with ether then neutralized with 1 N HCl resulting in a cloudy solution. The suspension was then extracted into ether. The resulting organic layer was then washed with water and brine followed by drying over magnesium sulfate and concentrated in vacuo, resulting in 1.37 g of a white powder (86% yield). <sup>1</sup>H NMR (300 MHz, CDCl<sub>3</sub>)  $\delta$  8.88 (d, 1H,  $J_1 = 7$  Hz), 7.48 (t, 1H,  $J = 8$  Hz), 7.08 (t, 1H,  $J = 6$  Hz), 6.96 (d, 1H,  $J = 8$  Hz), 5.83 (s, 2H), 3.98 (s, 3 Hz).

**2-(2-Methoxyphenylbenzaldehyde), 3.** A round-bottom flask was charged with argon, benzene, 2-bromobenzaldehyde (760 mg, 4.11 mmol), and compound **2** (750 mg, 4.93 mmol) at room temperature. To the flask, Pd(PPh<sub>3</sub>)<sub>4</sub> (94 mg, 0.08 mmol) and 2 mL of 2 M K<sub>2</sub>CO<sub>3</sub> were added along with a reflux condenser. The reaction was allowed to react overnight under reflux. Upon cooling, 5 mL of 30% H<sub>2</sub>O<sub>2</sub> was added and stirred for 30 min. The reaction mixture was extracted into ether and washed with 20 mL of water followed by 20 mL of brine. The organic layer was dried over magnesium sulfate and concentrated in vacuo. The resulting oil was purified by column chromatography (5:1 hexanes/ethyl acetate) to give a white solid (837 mg, 96% yield). <sup>1</sup>H NMR (400 MHz, CDCl<sub>3</sub>)  $\delta$  9.93 (s, 1H), 8.14 (dd, 1H,  $J_1 = 8$  Hz,  $J_2 = 1$  Hz), 7.79 (d, 1H,  $J_1 = 8$  Hz,  $J_2 = 1$  Hz), 7.62 (t, 1H,  $J = 7$  Hz), 7.56 (m, 1H), 7.50 (d, 1H,  $J = 8$  Hz), 7.43 (dd, 1H,  $J_1 = 7$  Hz,  $J_2 = 1$  Hz), 7.23 (dt, 1H,  $J_1 = 7$  Hz,  $J_2 = 1$  Hz), 7.12 (d, 1H,  $J = 8$  Hz), 3.88 (s, 3H). LR-MS (ESI): calculated = 212.2; actual = 212.0.

**2'-Bromomethyl-2-methoxy-biphenyl, 4.** A round-bottom flask was charged with argon, THF (25 mL), and **3** (0.55 mmol). LiAlH<sub>4</sub> was subsequently added in small portions, and the reaction mixture was allowed to stir for 1 h. The reaction was quenched with 1 N HCl (10 mL) and diluted with ethyl ether. The reaction was washed with 10 mL portions of sodium sulfate, water, and brine, respectively. Finally, the organic layer was dried over magnesium sulfate and concentrated in vacuo. The resulting product was then taken up in 10 mL of chloroform under an atmosphere of argon. Phosphorus tribromide (54.7 mg, 0.20 mmol, 19  $\mu$ L) was added as a 1 mL chloroform solution and stirred for 2 h. The reaction was quenched with 10 mL of water followed by a wash of 10 mL of sodium bicarbonate, water, and brine, respectively. The organic layer was dried over magnesium sulfate and concentrated in vacuo. The product was carried on to the formation of compound **1a** without purification.

**1-(2'-Methoxy-biphenyl-2-ylmethyl)-pyridinium Bromide, 1a.** In a small vial pyridine (1 mL) was added to compound **4** (100 mg, 0.4 mmol) and was allowed to sit until a white precipitate formed. The solution was diluted with ethyl ether and filtered to recover a white solid. The solid was purified by washing with ethyl ether and dried under reduced pressure to recover the desired product quantitatively. <sup>1</sup>H NMR (500 MHz, D<sub>2</sub>O pH 1)  $\delta$  8.25 (t, 1H,  $J = 7$  Hz), 8.09 (d, 1H,  $J = 8$  Hz), 7.63 (t, 1H,  $J = 7$  Hz), 7.57 (m, 1H), 7.44 (m, 2H), 7.30 (t, 1H,  $J = 8$  Hz), 7.10 (m, 1H), 6.86 (m, 2H), 6.79 (d, 1H,  $J = 7$  Hz), 4.88 (q, 2H,  $J = 15$  Hz), 3.34 (s, 3H); <sup>13</sup>C NMR (75 MHz, D<sub>2</sub>O pH 1)  $\delta$  155, 145, 144, 138, 131, 131, 130, 130, 130, 128, 127, 127, 121, 111, 63, 55. LR-MS (FAB): calculated = 276.4; actual = 276.2.

**(2-Bromophenyl)-pyridin-2-yl-methanol, 6b.** A dry round-bottom flask charged with argon and a stirbar was filled with isopropylmagnesium chloride (2 M in THF, 5.2 mL, 10.4 mmol) followed by the dropwise addition of 2-bromopyridine (1 mL, 10.4 mmol) while stirring at room temperature. After 1 h 2-bromobenzaldehyde (1.34 mL, 11.5 mmol) was added and stirred for another 2 h while monitored by TLC.

(14) Pangborn, A. B.; Giardello, M. A.; Grubbs, R. H.; Rosen, R. K.; Timmers, F. J. *Organometallics* **1996**, *15*, 1518–1520.

(15) SYBYL 6.9, Tripos Inc. 1699 South Hanley Road, St. Louis, Missouri 63144, USA.

The reaction was quenched with 10 mL of 1 N HCl. The aqueous layer is washed with ether and then neutralized with 1 N NaOH resulting in a cloudy solution. The suspension was then extracted into ether. The resulting organic layer was then washed with water and brine followed by drying over magnesium sulfate and concentrated in vacuo, recovering 1.45 g of an off-white colored powder (52% yield).  $^1\text{H NMR}$  (400 MHz,  $\text{CDCl}_3$ )  $\delta$  8.56 (d, 1H,  $J = 5$  Hz), 7.61 (t, 1H,  $J = 7$  Hz), 7.56 (d, 1H,  $J_1 = 7$  Hz), 7.33 (d, 1H,  $J = 8$  Hz), 7.23 (m, 2H), 7.11 (t, 1H,  $J = 8$  Hz), 6.73 (d, 1H,  $J = 2$  Hz), 5.48 (d, 1H,  $J = 2$  Hz). LR-MS (ESI): calculated = 264.1; actual = 264.0.

**(2-Bromophenyl)-pyridin-3-yl-methanol, 6c.** See synthesis of **6b**. 69% yield.  $^1\text{H NMR}$  (300 MHz,  $\text{CDCl}_3$ )  $\delta$  8.66 (s, 1H), 8.50 (d, 1H,  $J = 5$  Hz), 7.70 (dt, 1H,  $J_1 = 7$  Hz,  $J_2 = 2$  Hz), 7.61 (dd, 1H,  $J_1 = 7$  Hz,  $J_2 = 2$  Hz), 7.56 (d, 1H,  $J = 7$  Hz), 7.38 (t, 1H,  $J = 2$  Hz), 7.26 (m, 1H), 7.19 (t, 1H,  $J_1 = 7$  Hz,  $J_2 = 2$  Hz), 6.35 (s, 1H). LR-MS (ESI): calculated = 264.1; actual = 264.0.

**(2-Bromophenyl)-pyridin-4-yl-methanol, 6d.** In a separatory funnel, 4-bromopyridine hydrochloride (2.5 g, 12.8 mmol) was deprotonated with 20 mL of 2 M  $\text{K}_2\text{CO}_3$  and extracted into 20 mL of dichloromethane. The organic layer was dried over  $\text{MgSO}_4$  and evaporated. The resulting oil was taken up into 20 mL of THF in a round-bottom flask and placed under an atmosphere of nitrogen. While stirred at room temperature, isopropylmagnesium chloride (2 M in THF, 6.4 mL, 12.8 mmol) was added dropwise and stirred for 1 h. After 1 h, 2-bromobenzaldehyde (1.58 mL, 12.8 mmol) was added and stirred for another 2 h while monitored by TLC. The reaction was quenched with 10 mL of 1 N HCl. The aqueous layer is washed with ether and then neutralized with 1 N NaOH resulting in a cloudy solution. The suspension was then extracted into ether. The resulting organic layer was then washed with water and brine followed by drying over magnesium sulfate and concentrated in vacuo, recovering 1.05 g of an off-white colored powder (31% yield).  $^1\text{H NMR}$  (300 MHz,  $\text{CDCl}_3$ )  $\delta$  8.54 (d, 2H,  $J = 6$  Hz), 7.57 (d, 1H,  $J_1 = 8$  Hz,  $J_2 = 2$  Hz), 7.46 (d, 1H,  $J_1 = 7$  Hz,  $J_2 = 2$  Hz), 7.35 (m, 3H), 7.18 (t, 1H,  $J_1 = 7$  Hz,  $J_2 = 2$  Hz), 6.24 (s, 1H).

**Acetic Acid (2-Bromo-phenyl)-pyridin-2-yl-methyl Ester, 7b.** A round-bottom flask charged with anhydrous methylene chloride, compound **6a** (394 mg, 1.49 mmol), acetic anhydride (167  $\mu\text{L}$ , 181 mg, 1.78 mmol), pyridine (143  $\mu\text{L}$ , 140 mg, 1.78 mmol), and DMAP (36 mg, 0.298 mmol) and stirred overnight at room temperature. The reaction mixture was quenched with water and adjusted to neutral pH. The water was extracted with methylene chloride, and the organic layer was dried over magnesium sulfate and concentrated in vacuo. The product was purified by column chromatography with 1:1 hexanes/ethyl acetate as the mobile phase resulting in 122 mg of a yellow oil (52% yield).  $^1\text{H NMR}$  (300 MHz,  $\text{CDCl}_3$ )  $\delta$  8.63 (d, 1H,  $J = 5$  Hz), 7.69 (t, 1H,  $J_1 = 8$  Hz,  $J_2 = 2$  Hz), 7.57 (d, 1H,  $J_1 = 2$  Hz,  $J_2 = 2$  Hz), 7.49 (d, 1H,  $J_1 = 8$  Hz,  $J_2 = 2$  Hz), 7.43 (d, 1H,  $J = 3$  Hz), 7.33 (t, 1H,  $J = 7$  Hz), 7.21 (m, 3H), 2.20 (s, 3H). LR-MS (CI): calculated = 305.0; actual = 306.0.

**Acetic Acid (2-Bromo-phenyl)-pyridin-3-yl-methyl Ester, 7c.** See synthesis of **7b**. (84% yield).  $^1\text{H NMR}$  (300 MHz,  $\text{CDCl}_3$ )  $\delta$  8.66 (s, 1H), 8.70 (d, 1H,  $J = 5$  Hz), 7.70 (dt, 1H,  $J_1 = 8$  Hz,  $J_2 = 2$  Hz), 7.57 (d, 1H,  $J = 8$  Hz), 7.52 (d, 1H,  $J = 8$  Hz), 7.43 (t, 1H,  $J = 7$  Hz), 7.29 (m, 1H), 7.20 (m, 2H), 2.17 (s, 3H). LR-MS (ESI): calculated = 305.0; actual = 305.0.

**Acetic Acid (2-Bromo-phenyl)-pyridin-4-yl-methyl Ester, 7d.** See synthesis of **7b**. 84% yield.  $^1\text{H NMR}$  (300 MHz,  $\text{CDCl}_3$ )  $\delta$  8.73 (d, 2H,  $J = 6$  Hz), 7.74 (d, 1H,  $J_1 = 8$  Hz,  $J_2 = 1$  Hz), 7.50 (m, 2H), 7.42 (d, 1H,  $J = 6$  Hz), 7.35 (m, 1H), 7.31 (s, 2H), 5.44 (s, 3H).

**2-Bromobenzyl-2-pyridine, 8b.** In a round-bottom flask charged with Ar and a stirbar was filled **4a** (167 mg, 0.55 mmol) and *t*-BuOH (61 mg, 0.8 mmol, 78  $\mu\text{L}$ ) in 5 mL of THF. This was followed by the addition of  $\text{SmI}_2$  (1.6 mmol, 16.4 mL, 0.1 M in THF) dropwise over approximately 10 min. The mixture was stirred for 2 h while monitored by TLC. The reaction was quenched with water and extracted with

ether followed by washes with water and brine. The organic layer was dried over magnesium sulfate and concentrated in vacuo. The resulting oil was purified by column chromatography (10:1 hexanes/ethyl acetate) to give 56 mg of product (46% yield).  $^1\text{H NMR}$  (400 MHz,  $\text{CDCl}_3$ )  $\delta$  8.57 (d, 1H,  $J = 4$  Hz), 7.58 (m, 2H), 7.27 (m, 2H), 7.12 (m, 3H), 4.32 (s, 2H). LR-MS (ESI): calculated = 248.1; actual = 248.0.

**2-Bromobenzyl-3-pyridine, 8c.** See synthesis of **8b**. 66% yield.  $^1\text{H NMR}$  (300 MHz,  $\text{CDCl}_3$ )  $\delta$  8.50 (m, 2H), 7.59 (d, 1H,  $J = 7$  Hz), 7.40 (d, 1H,  $J = 8$  Hz), 7.18 (m, 4H), 4.12 (s, 2H).

**2-Bromobenzyl-4-pyridine, 8d.** See synthesis of **8b**.  $^1\text{H NMR}$  (300 MHz,  $\text{CDCl}_3$ )  $\delta$  8.64 (d, 2H,  $J = 6$  Hz), 7.73 (d, 1H,  $J = 8$  Hz), 7.74 (m, 1H), 7.26 (m, 4H), 4.25 (s, 2H).

**2-(2'-Methoxy-biphenyl-2-ylmethyl)-Pyridine, 1b.** A round-bottom flask was filled with argon, 20 mL of benzene, compound **8b** (102 mg, 0.41 mmol), and compound **2** (66 mg, 0.49 mmol) at room temperature. To the flask  $\text{Pd}(\text{PPh}_3)_4$  (23 mg, 0.02 mmol) and 2 mL of 2 M  $\text{K}_2\text{CO}_3$  were added. The reaction was allowed to react overnight under reflux. Upon cooling, 5 mL of 30%  $\text{H}_2\text{O}_2$  was added and stirred for 30 min. The reaction mixture was extracted into ether and washed with 20 mL of water followed by 20 mL of brine. The organic layer was dried over magnesium sulfate and concentrated in vacuo. The resulting oil was purified by column chromatography (10:1 hexanes/ethyl acetate) to give a yellow oil.  $^1\text{H NMR}$  (500 MHz,  $\text{D}_2\text{O}$  pH 1)  $\delta$  8.1 (d, 1H,  $J = 5$  Hz), 8.047 (t, 1H), 7.536 (t, 1H), 7.405 (s, 1H), 7.329 (s, 1H), 7.18 (m, 2H), 7.073 (d, 1H,  $J = 4.5$  Hz), 6.751 (m, 3H), 4.155 (dd, 2H), 3.361 (s, 3H);  $^{13}\text{C NMR}$  (100 MHz,  $\text{D}_2\text{O}$  pH 1)  $\delta$  155, 155, 146, 140, 138, 134, 131, 131, 130, 130, 128, 128, 128, 127, 124, 121, 111, 55, 38. LR-MS (ESI): calculated = 275.3; actual = 275.1.

**3-(2'-Methoxy-biphenyl-2-ylmethyl)-pyridine, 1c.** See synthesis of **1b**.  $^1\text{H NMR}$  (500 MHz,  $\text{D}_2\text{O}$  pH 1)  $\delta$  8.31 (d, 1H,  $J = 6$  Hz), 7.72 (d, 1H,  $J = 8$  Hz), 7.68 (s, 1H), 7.55 (q, 1H,  $J = 6$  Hz), 7.33 (d, 1H,  $J = 7$  Hz), 7.21 (m, 2H), 7.11 (t, 1H,  $J = 7$  Hz), 6.81 (d, 2H,  $J = 7$  Hz), 6.75 (m, 2H), 6.61 (dd, 1H,  $J_1 = 8$  Hz,  $J_2 = 2$  Hz), 3.84 (q, 2H,  $J = 15$  Hz), 3.32 (s, 3H);  $^{13}\text{C NMR}$  (75 MHz,  $\text{D}_2\text{O}$  pH 1)  $\delta$  155, 155, 146, 140, 138, 138, 136, 131, 130, 130, 129, 128, 128, 127, 126, 124, 121, 54, 36. LR-MS (ESI): calculated = 275.3; actual = 275.1.

**4-(2'-Methoxy-biphenyl-2-ylmethyl)-pyridine, 1d.** See synthesis of **1b** (22% yield).  $^1\text{H NMR}$  (500 MHz,  $\text{D}_2\text{O}$  pH 1)  $\delta$  8.27 (d, 2H,  $J = 6$  Hz), 7.42 (d, 1H,  $J = 7$  Hz), 7.32 (m, 6H), 7.09 (d, 1H,  $J = 7$  Hz), 6.86 (d, 1H,  $J = 8$  Hz), 6.82 (m, 2H), 4.08 (q, 2H,  $J = 15$  Hz), 3.45 (s, 3H).  $^{13}\text{C NMR}$  (75 MHz,  $\text{D}_2\text{O}$  pH 1)  $\delta$  163, 155, 139, 138, 136, 130, 129, 129, 128, 127, 121, 111, 55, 40. LR-MS (ESI): calculated = 275.3; actual = 275.1.

**2-Bromobenzyl-N-pyridine Bromide, 9a.** A round-bottom flask was filled with argon, 20 mL of THF, 2-bromobenzaldehyde (8.56 mmol), and sodium cyanoborohydride (0.538 g, 8.6 mmol). The reaction was allowed to stir for 1 h, then quenched with 1 N HCl (10 mL), and diluted with diethyl ether. The ether layer was washed with water and brine, dried over magnesium sulfate, and concentrated in vacuo. The resulting white solid was taken up into 20 mL of chloroform under an argon atmosphere. Phosphorus tribromide was added (271  $\mu\text{L}$ ; 2.85 mmol), and the reaction was allowed to stir for 1.5 h. The reaction was quenched with 10 mL of water, followed by washes of sodium bicarbonate, water, and brine. The organic layer was dried with magnesium sulfate and concentrated in vacuo to give a yellow oil. Pyridine (2 mL) was added, and the solution was allowed to stand until a white precipitate formed. The precipitated product was filtered and washed several times with diethyl ether (1.27 g, 60% overall yield).  $^1\text{H NMR}$  (500 MHz,  $\text{D}_2\text{O}$ )  $\delta$  8.736 (d, 2H,  $J = 6$  Hz), 8.423 (t, 1H,  $J = 7.5$  Hz), 7.919 (t, 2H,  $J_1 = 7$  Hz,  $J_2 = 8$  Hz), 7.54 (d, 1H,  $J = 8$  Hz), 7.452 (d, 1H,  $J = 7.5$  Hz), 7.357 (t, 1H,  $J = 7.5$  Hz), 7.252 (t, 1H,  $J_1 = 8$  Hz,  $J_2 = 7.5$  Hz), 5.763 (s, 2H).

**Synthesis of Control Compounds 9b–9d.** Purified compounds **8b–8d** were placed in scintillation vials with 5 mL of  $\text{H}_2\text{O}$  and titrated to pH 1 with 50%  $\text{HBF}_4$ . The aqueous solutions were subsequently frozen and lyophilized in preparation for NMR analysis in  $\text{D}_2\text{O}$ .

**2-Bromobenzyl-2-pyridine, 9b.**  $^1\text{H}$  NMR (500 MHz,  $\text{D}_2\text{O}$ )  $\delta$  8.501 (d, 1H,  $J = 6$  Hz), 8.295 (t, 1H,  $J = 8$  Hz), 7.762 (t, 1H,  $J = 7$  Hz), 7.551 (d, 2H,  $J = 8$  Hz), 7.330 (m, 2H), 7.187 (t, 1H,  $J_1 = 7$  Hz,  $J_2 = 7.75$  Hz), 4.433 (s, 2H).

**2-Bromobenzyl-3-pyridine, 9c.**  $^1\text{H}$  NMR (400 MHz,  $\text{D}_2\text{O}$ )  $\delta$  8.31 (d, 1H,  $J = 6$  Hz), 8.287 (s, 1H), 8.109 (d, 1H,  $J = 8$  Hz), 7.640 (t, 1H,  $J_1 = 7.2$ ,  $J_2 = 6.4$ ), 7.355 (d, 1H,  $J = 8$  Hz), 7.125 (m, 2H), 6.953 (t, 1H,  $J = 7.6$  Hz), 4.056 (s, 2H).

**2-Bromobenzyl-4-pyridine, 9d.**  $^1\text{H}$  NMR (500 MHz,  $\text{D}_2\text{O}$ )  $\delta$  8.446 (d, 2H,  $J = 7$  Hz), 7.671 (d, 2H,  $J = 6.5$  Hz), 7.530 (d, 1H,  $J = 8$  Hz), 7.281 (m, 2H), 7.135 (t, 1H,  $J_1 = 8$  Hz,  $J_2 = 7$  Hz), 4.300 (s, 2H).

**Synthesis of *N*-Methyl-2-(2'-methoxy-biphenyl-2-ylmethyl)-pyridinium Methyl Sulfate (*N*-Me-1b).** In a 1 dram vial compound **1b** (40 mg, 0.14 mmol) was combined with dimethyl sulfate (25 mg, 0.2 mmol) in benzene and reacted for 2 h. The reaction was quenched with ether, and the precipitate was collected through filtration and washed with ether to recover a white solid.  $^1\text{H}$  NMR (300 MHz,  $\text{D}_2\text{O}$ )  $\delta$  8.37 (d, 1H,  $J = 6$  Hz), 8.03 (t, 1H,  $J = 8$  Hz), 7.58 (t, 1H,  $J = 7$  Hz), 7.35 (m, 3H), 7.26 (m, 2H), 7.16 (m, 1H), 6.86 (m, 3H), 4.23 (q, 2H,  $J = 15$  Hz), 3.77 (s, 3H), 3.60 (s, 3H), 3.46 (s, 3H).

**Synthesis of *N*-Methyl-3-(2'-methoxy-biphenyl-2-ylmethyl)-pyridinium Iodide (*N*-Me-1c):** In a 1 dram vial compound **1c** (25 mg, 0.1 mmol) was combined with 100  $\mu\text{L}$  of iodomethane and reacted for 2 h. The reaction was quenched with ether, and the precipitate was collected through filtration and washed with ether to recover a yellowish solid.  $^1\text{H}$  NMR (400 MHz,  $\text{D}_2\text{O}$ )  $\delta$  8.33 (d, 1H,  $J = 6$  Hz), 7.78 (d, 1H,  $J = 8$  Hz), 7.69 (s, 1H), 7.60 (t, 1H,  $J = 7$  Hz), 7.47 (dd, 1H,  $J_1 = 7$  Hz,  $J_2 = 2$  Hz), 7.35 (m, 3H), 7.11 (d, 1H,  $J_1 = 7$  Hz,  $J_2 = 2$  Hz), 6.88 (m, 3H), 3.97 (q, 2H,  $J = 15$  Hz), 3.99 (s, 3H), 3.44 (s, 3H).

**Synthesis of *N*-Methyl-4-(2'-methoxy-biphenyl-2-ylmethyl)-pyridinium Iodide (*N*-Me-1d):** See synthesis of *N*-Me-1c.  $^1\text{H}$  NMR (400 MHz,  $\text{D}_2\text{O}$ )  $\delta$  8.76 (s, 2H), 7.40 (m, 1H), 7.36 (m, 2H), 7.29 (m, 1H), 7.22 (s, 2H), 7.13 (dd, 1H,  $J_1 = 7$  Hz,  $J_2 = 2$  Hz), 6.90 (d, 1H,  $J = 9$  Hz), 6.84 (m, 2H), 4.09 (s, 3H), 4.05 (q, 2H,  $J = 15$  Hz).

**Synthesis of *N*-Methyl-2-bromobenzyl-2-pyridinium Iodide (*N*-Me-9b):** See synthesis of *N*-Me-1c.  $^1\text{H}$  NMR (500 MHz,  $\text{D}_2\text{O}$ )  $\delta$  8.577 (d, 1H,  $J = 6$  Hz), 8.298 (t, 1H,  $J_1 = 8$  Hz,  $J_2 = 6$  Hz), 7.763 (d, 1H,  $J = 8.5$  Hz), 7.735 (t, 1H,  $J_1 = 9.5$  Hz,  $J_2 = 7$ ), 7.572 (d, 1H,  $J = 8$  Hz), 7.265 (t, 1H,  $J_1 = 7.5$  Hz,  $J_2 = 6.5$  Hz), 7.142 (t, 1H,  $J_1 = 7.5$  Hz,  $J_2 = 6.5$  Hz), 7.07 (d, 1H,  $J = 6.5$  Hz), 5.291 (s, 2H), 4.12 (s, 3H).

**Synthesis of *N*-Methyl-2-bromobenzyl-3-pyridinium Iodide (*N*-Me-9c):** See synthesis of *N*-Me-1c.  $^1\text{H}$  NMR (400 MHz,  $\text{D}_2\text{O}$ )  $\delta$  8.50 (d, 1H,  $J = 6$  Hz), 8.45 (s, 1H), 8.22 (d,  $J = 8$  Hz), 7.80 (t, 1H,  $J = 8$  Hz), 7.40 (m, 2H), 7.18 (t, 1H,  $J_1 = 7$  Hz,  $J_2 = 2$  Hz), 4.25 (s, 2H), 4.19 (s, 3H).

**Synthesis of *N*-Methyl-2-bromobenzyl-4-pyridinium Iodide (*N*-Me-9d):** See synthesis of *N*-Me-1c.  $^1\text{H}$  NMR (500 MHz,  $\text{D}_2\text{O}$ )  $\delta$  8.412 (d, 2H,  $J = 6.5$  Hz), 7.601 (d, 2H,  $J = 6$  Hz), 7.488 (d, 1H,  $J = 8$  Hz), 7.273 (m, 2H), 7.110 (t, 1H,  $J_1 = 8$  Hz,  $J_2 = 7$  Hz), 4.231 (s, 2H), 4.124 (s, 3H).

**NMR Data Acquisition.** A spectrum of each sample was taken at 10  $^\circ\text{C}$  temperature intervals from 298 K to coalescence on a Bruker 300AMX NMR. Temperature calibration was done through the use of the known temperature dependence of ethylene glycol chemical shifts; as a result, the spectrometer was calibrated to an accuracy of  $\pm 0.2$  K. The sample was allowed to equilibrate at a given temperature for at least 5 min before data acquisition. Temperature stability was assured by NMR temperature calibration before and after each experiment acquisition. Near the reported temperature, spectra were obtained at decreased temperature intervals once equilibration had been achieved. Water suppression NMR techniques were employed, when possible, to maximize the signal-to-noise of the spectrum. Although there were changes in chemical shift of the methylene hydrogens with changes in temperature, these shifts were linear and were accounted for in the fitting of the data.

**NMR Data Analysis.** Each spectrum was analyzed using the program gNMR from Cherwell Scientific Publishing. The spectrum was converted from a WIN-NMR file by gNMR. The methoxy protons were simulated to determine the baseline line width. The line width was then used to iterate on the diastereotopic methylene hydrogens allowing us to determine the rate constant for rotation about the biaryl bond. Each sample was acquired and analyzed at least twice to ensure accuracy, with a standard deviation of 0.01 kcal mol $^{-1}$  in all cases. The reported  $\Delta G^\ddagger$  was determined from extrapolation of the data collected near coalescence to 352 K. The error in the rate constant was determined to be less than 5%, which corresponds to a total error of  $\pm 0.04$  kcal mol $^{-1}$  through propagation of errors in both  $k$  and  $T$ .

**Acknowledgment.** This work was supported by an NSF Career Award (CHE-0094068). N.T.C. thanks the Francis C. and William P. Smallwood Foundation and the UNC Office of Undergraduate Research for support.

**Supporting Information Available:** NMR spectra of compounds **1a–d**, **9a–d**, **N-Me-1b–d**, and **N-Me-9b–d**. This material is available free of charge via the Internet at <http://pubs.ac.org>.

JA0498538